Supporting information

for

Electrochemical activation of CO_2 by MOF-(Fe, Ni, Mn) derivatives of 5-aminoisophthalic acid and the thiazole group influence on its catalytic activity

Elvis Robles-Marín, Marcos Flores-Alamo and Juventino J. Garcia*

Facultad de Química, Universidad Nacional Autónoma de México, Mexico City, 04510, Mexico.

juvent@unam.mx

Table of Contents

List of Tables

List of Figures

1. Materials and general methods

1.1 General considerations

Unless otherwise stated, all processes were performed using standard Schlenk techniques in an inter-gas/vacuum double manifold or under argon atmosphere (Praxair 99.998); this used a MBraun Unilab SP glovebox (< 1 ppm H_2O and O_2). All liquid reagents were purchased as reagent grade and degassed before use. Regular THF (J.T. Baker) was dried and degassed in a MB-SPS-800. Water was distilled, deionized, and degassed under an argon flow before use. *5-aminoisophtalic acid* (94 % purity), *2-thiozolecarboxaldehyde* (Sigma-Aldrich, reagent grade 97%), $FeCl_3 \cdot 6H_2O$ (reagent grade 97%), $NiCl_2 \cdot 6H_2O$ (99% purity), $MnCl_2 \cdot 4H_2O$ (98% purity), *N,N-Dimethylacetamide* (Sigma-Aldrich, >99 % purity). Deuterated solvents for NMR experiments were purchased from Cambridge Isotope Laboratories and were stored under 4 Å molecule sieves for 24 h before use. NMR spectra were recorded at room temperature on a JEOL 600 MHz. All reagents for the catalytic reactions were loaded in the indicated glove box. IR spectra were taken on the *PerkinElmer* FT-IR Spectrometrer Frontier. Shelton CT06484. The electrochemical equipment used was *Gamry Instruments*, Interface1000, Potentiostat/Galvanostat/ZRA 07067. The electrochemical cell used was Jacket-Eurocell Kit. The luminescence experiments were carried out in a kimmon He-Cd laser equipment at λ = 325 nm excitation, with a photomultiplier of the laser is SpectraPro 2500i, and the UV-vis spectra were taken in Filmetrics F10-RT-UV. The thermogravimetric studies were carried out on TGA Q5000 IR equipment.

2. X-ray Crystallography

Suitable single crystals of **LH_2**, **1**, and **5** were mounted on a glass fiber and crystallographic data were collected with an Oxford Diffraction Gemini "A" diffractometer with a CCD area detector ($\lambda_{MoK\alpha}$ = 0.71073 Å, monochromator: graphite) at 120 K. Unit cell parameters were determined with a set of three runs of 15 frames (1° in ω). The double pass method of scanning was used to exclude any noise. The collected frames were integrated by using an orientation matrix determined from the narrow frame scans. CrysAlisPro and CrysAlisRED software packages [1] were used for data collection and integration. Analysis of the integrated data did not reveal any decay. Collected data were corrected for absorption effects by an analytical numeric absorption correction [2] using a multifaceted crystal model based on expressions upon the Laue symmetry with equivalent reflections. Structure solution and refinement were carried out with the programs SHELXS-2018 [3] and SHELXL-2018 [4] respectively. WinGX v2020.2 [5] and Mercury CSD 4.1.0 software [6] were used to prepare material for publication. Full-matrix least-squares refinement was carried out by minimizing $(Fo^2 - Fc^2)^2$. All nonhydrogen atoms were refined anisotropically. H atoms of the water (O-H) and amine (N-H) groups were located in a difference map and refined isotropically with Uiso(H) of 1.5 Ueq and 1.2 Ueq for H-O and N-H respectively. Hydrogen atoms attached to carbon atoms were placed in geometrically idealized positions and refined as riding on their parent atoms, with C—H = 0.95 – 99 Å with Uiso (H) = 1.2Ueq(C) for aromatic and methylene groups. In compound **5**, C9, C9 and

C9A, C10A are disordered over two sites with occupancies of 0.60:40. Crystal data and experimental details of the structure determination are listed in Table S1. Powder X-ray diffraction pattern was obtained on a D8-Advance equipped with Cu Ka radiation in the range $4° < 2\theta < 60°$, with a step size of 0.02° (2θ) and a count time of 2 s/step. Crystallographic data have been deposited at the Cambridge Crystallographic Data Center as supplementary material CCDC: 2103571-2103573. Copies of the data can be obtained free of charge on application to CCDC, 12 Union Road, Cambridge CB2 1EZ, UK. e-mail: deposit@ccdc.cam.ac.uk.

Table S1. Selected crystallographic data for **LH_2**, **1**, and **5**.

	LH_2	**1**	**5**
Empirical formula	$C_{12}\,H_{10}\,N_2\,O_4\,S$	$C_8\,H_9\,Fe\,N\,O_6$	$C_{12}\,H_8\,Mn\,N_2\,O_4\,S$
Formula weight	278.28	271.01	331.20
Temperature	120(2) K	119(2) K	120(2) K
Wavelength	0.71073 Å	0.71073 Å	0.71073 Å
Crystal system	Triclinic	Triclinic	Monoclinic
Space group	P-1	P-1	P 21/c
a (Å)	5.4648(8)	7.394(3)	8.7610(10)
b (Å)	10.4074(17)	8.345(3)	10.3491(14)
c (Å)	10.6121(19)	8.843(4)	14.860(2)
β (°)	81.501(14)	71.92(3)	91.067(13)
Volume ($Å^3$)	582.19(17)	461.1(3)	1347.1(3)
Z	2	2	4
Density (calculated)	1.587 Mg/m^3	1.952 Mg/m^3	1.633 Mg/m^3
Absorption coefficient	0.290 mm^{-1}	1.649 mm^{-1}	1.147 mm^{-1}
F(000)	288	276	668
Crystal size(mm^3)	0.31 x 0.15 x 0.05	0.46 x 0.18 x 0.15	0.23 x 0.11 x 0.08
Theta range for data collection	3.830 to 29.539°	3.384 to 29.439°	3.323 to 25.026 °
Reflections collected	6519	5074	2388
Independent reflections	2763 [R(int) = 0.0581]	2189 [R(int) = 0.0257]	2388 [R(int) = 0.1103]
Completeness to theta = 25.242°	99.8 %	99.8 %	99.8 %
Data / restraints / parameters	2763 / 0 / 174	2189 / 6 / 163	2388 / 3 / 177
Goodness-of-fit on F^2	1.017	1.061	1.116
R1 I ≥2σ (I)	0.0532	0.0306	0.0953
wR2 I ≥2σ (I)	0.1107	0.0628	0.2591

Table S2 Selected bond lengths (Å) and angles (º) for $\mathbf{LH_2}$

$\mathbf{LH_2}$			
S(1)-C(10)	1.715(3)	N(1)-C(3)	1.383(3)
S(1)-C(11)	1.719(2)	N(1)-C(12)	1.428(3)
O(1)-C(7)	1.313(3)	N(2)-C(11)	1.300(3)
O(2)-C(7)	1.225(3)	N(2)-C(9)	1.383(3)
O(3)-C(8)	1.325(3)	C(1)-C(6)	1.380(3)
O(4)-C(8)	1.210(3)	C(5)-C(6)	1.387(3)
C(10)-S(1)-C(11)	89.58(12)	C(3)-N(1)-C(12)	123.74(19)
C(11)-N(2)-C(9)	110.9(2)	O(2)-C(7)-O(1)	122.8(2)
O(2)-C(7)-O(1)	122.8(2)	O(2)-C(7)-C(1)	121.5(2)
O(4)-C(8)-O(3)	123.3(2)	O(4)-C(8)-C(5)	123.7(2)

Table S3 Selected bond lengths (Å) and angles (º) for **1**

1			
Fe(1)-O(1)	1.9916(16)	Fe(1)-O(1W)	2.1833(18)
Fe(1)-O(2)	2.0544(19)	Fe(1)-N(1)	2.291(2)
Fe(1)-O(3)	2.1194(16)	Fe(1)-O(4)	2.2959(19)
N(1)-H(1G)	0.913(16)	C(5)-N(1)	1.423(3)
N(1)-H(1F)	0.876(16)	C(7)-O(1)	1.265(2)
C(3)-C(8)	1.494(3)	C(8)-O(4)	1.248(2)
C(7)-O(2)	1.254(3)	C(8)-O(3)	1.278(3)
O(1)-Fe(1)-O(2)	101.82(7)	O(3)-Fe(1)-N(1)	89.78(7)
O(1)-Fe(1)-O(3)	160.91(6)	O(1W)-Fe(1)-N(1)	170.39(6)
O(2)-Fe(1)-O(3)	96.42(7)	O(1)-Fe(1)-O(4)	102.51(7)
O(1)-Fe(1)-O(1W)	95.89(7)	O(2)-Fe(1)-O(4)	155.67(6)
O(2)-Fe(1)-O(1W)	97.60(7)	O(3)-Fe(1)-O(4)	59.36(6)
O(3)-Fe(1)-O(1W)	87.15(7)	O(1W)-Fe(1)-O(4)	80.07(7)
O(1)-Fe(1)-N(1)	84.13(7)	N(1)-Fe(1)-O(4)	90.53(7)
O(2)-Fe(1)-N(1)	91.79(7)	C(5)-N(1)-Fe(1)	112.09(13)

Table S4 Selected bond lengths (Å) and angles (º) for **5**

5			
Mn(1)-O(4)	2.098(7)	S(1)-C(10)	1.63(3)
Mn(1)-O(3)	2.112(7)	S(1)-C(11)	1.707(13)
Mn(1)-N(2)	2.156(9)	S(1)-C(10A)	1.78(2)
Mn(1)-O(2)	2.157(7)	O(1)-C(7)	1.254(13)
Mn(1)-O(1)	2.163(7)	O(2)-C(7)#1	1.229(13)
Mn(1)-Mn(1)#1	3.073(3)	O(3)-C(8)	1.257(13)
N(1)-C(3)	1.366(15)	N(1)-C(12)#2	1.439(13)
O(4)-Mn(1)-O(3)	155.8(3)	N(2)-Mn(1)-O(1)	106.0(3)
O(4)-Mn(1)-N(2)	106.2(3)	O(2)-Mn(1)-O(1)	154.5(3)
O(3)-Mn(1)-N(2)	97.9(3)	O(4)-Mn(1)-Mn(1)#1	77.4(2)
O(4)-Mn(1)-O(2)	86.3(3)	O(3)-Mn(1)-Mn(1)#1	79.3(2)
O(3)-Mn(1)-O(2)	87.3(3)	N(2)-Mn(1)-Mn(1)#1	157.7(3)
N(2)-Mn(1)-O(2)	99.5(3)	O(2)-Mn(1)-Mn(1)#1	58.4(2)
O(4)-Mn(1)-O(1)	86.7(3)	O(1)-Mn(1)-Mn(1)#1	96.2(2)
O(3)-Mn(1)-O(1)	89.1(3)	C(10)-S(1)-C(11)	91.8(10)

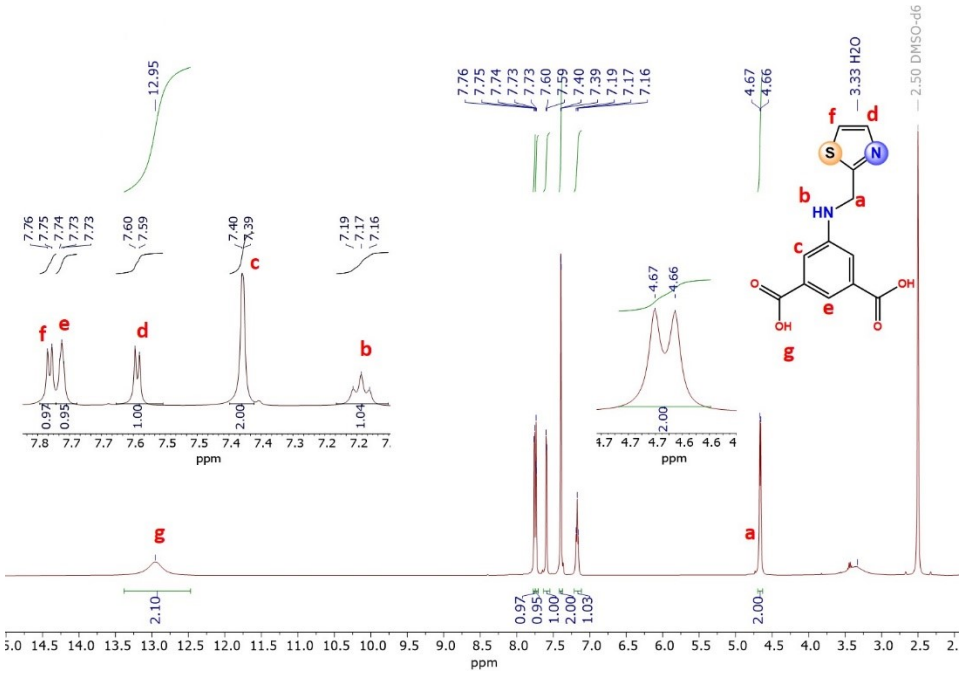

Figure S1 NMR-^{1}H spectrum of $\mathbf{LH_2}$.

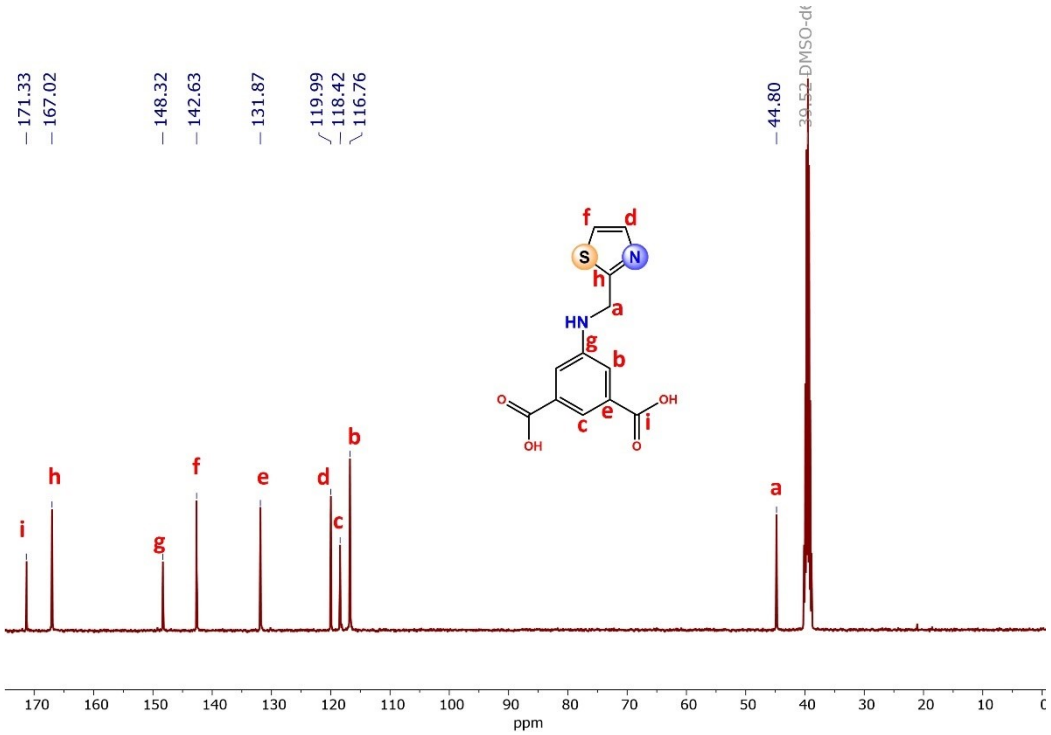

Figure S2 NMR-^{13}C spectrum of $\mathbf{LH_2}$.

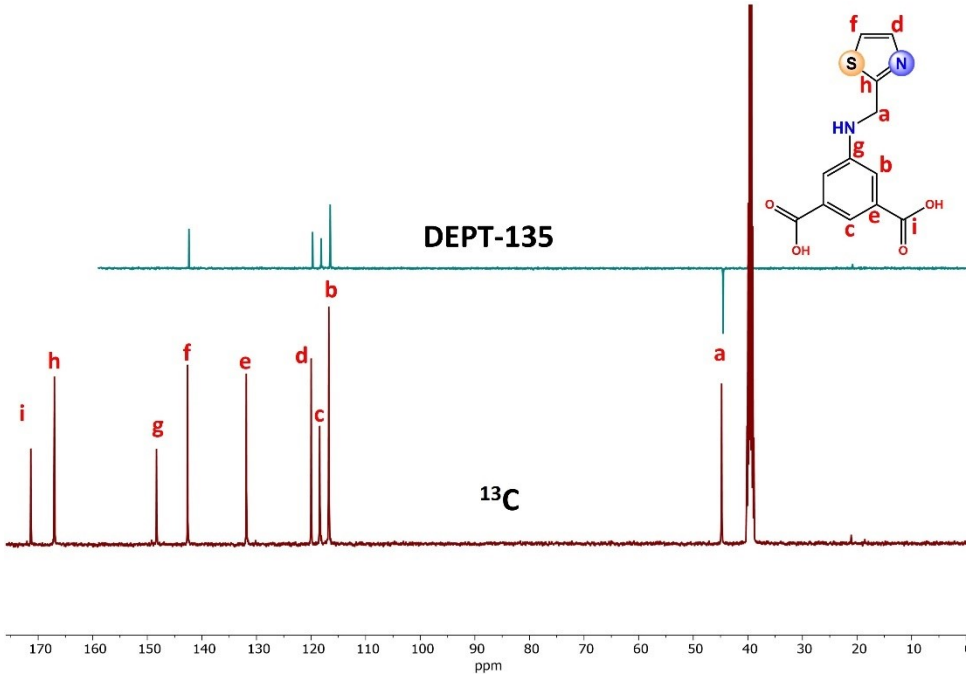

Figure S3 Comparison between NMR-^{13}C and DEPT-135 spectrums of ligand $\mathbf{LH_2}$.

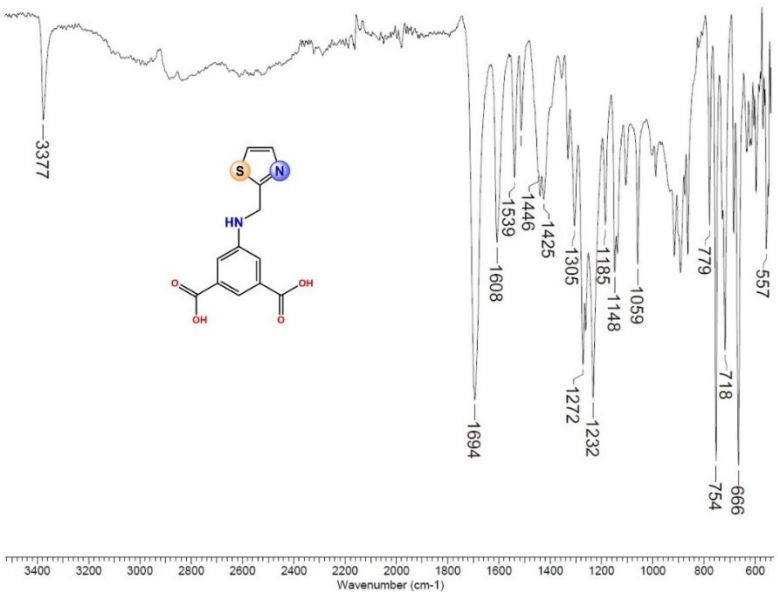
3377
1694
1608
1539
1446
1425
1305
1272
1232
1185
1148
1059
779
718
754
666
557
HN
S
N
OH
OH
O
O
3400 3200 3000 2800 2600 2400 2200 2000 1800 1600 1400 1200 1000 800 600
Wavenumber (cm-1)

(a)

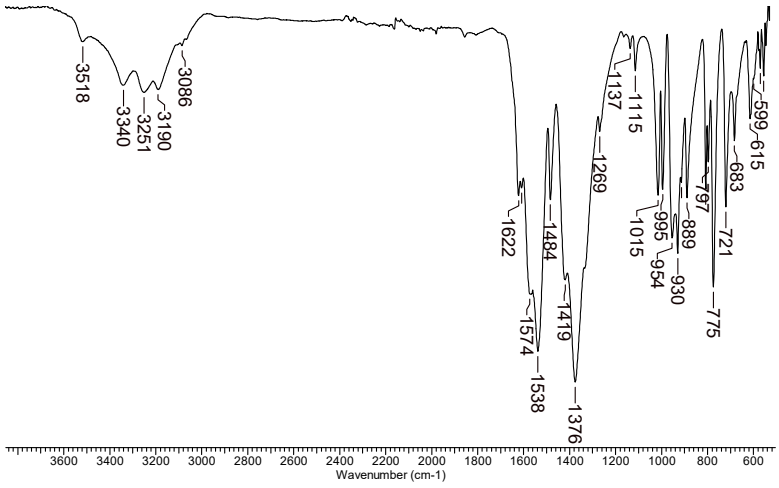
3518
3340
3251
3190
3086
1622
1574
1538
1484
1419
1376
1269
1137
1115
1015
995
954
930
889
797
775
721
683
615
599
3600 3400 3200 3000 2800 2600 2400 2200 2000 1800 1600 1400 1200 1000 800 600
Wavenumber (cm-1)

(b)

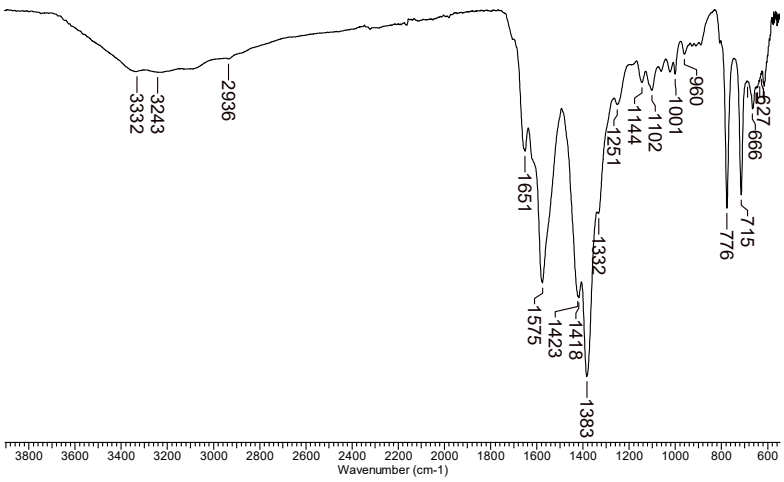
3332
3243
2936
1651
1575
1423
1418
1383
1332
1251
1144
1102
1001
960
927
776
715
666
3800 3600 3400 3200 3000 2800 2600 2400 2200 2000 1800 1600 1400 1200 1000 800 600
Wavenumber (cm-1)

(c)

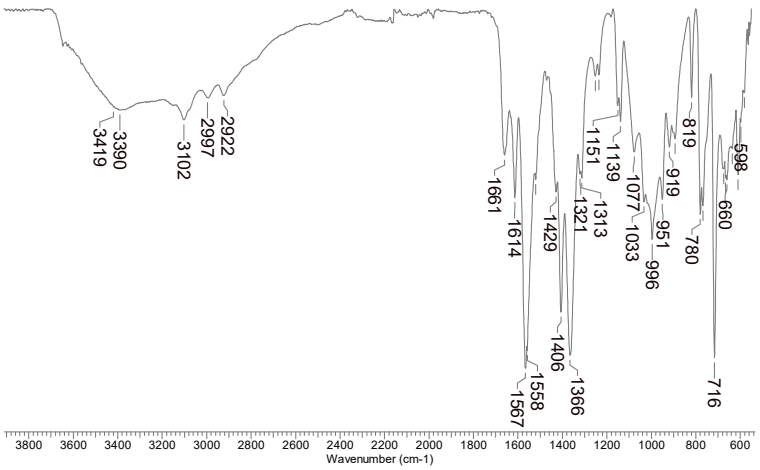

(d)

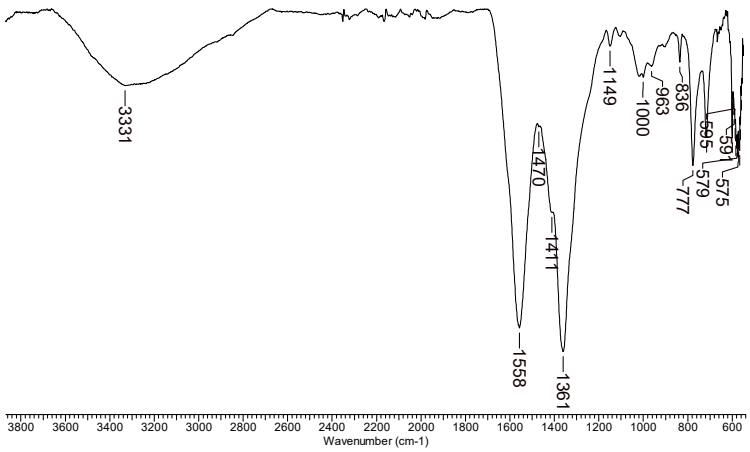

(e)

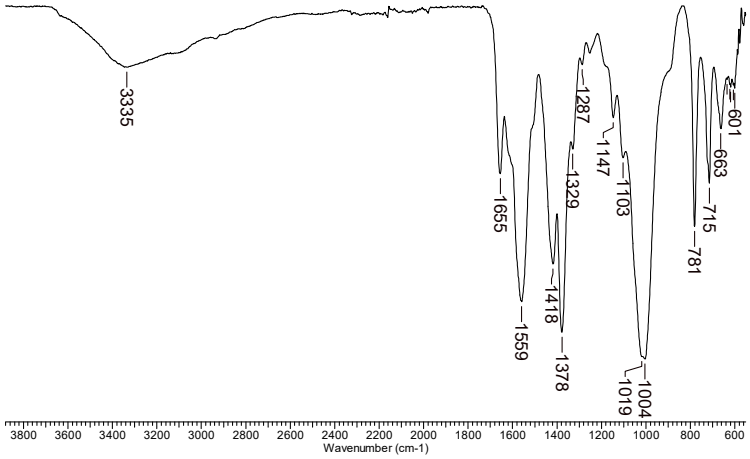

(f)

Figure S4 The IR spectra: (a) Ligand $\mathbf{LH_2}$ (b) complex **1**; (c) complex **2**; (d) complex **3**; (e) complex **4**; (f) complex **5**.

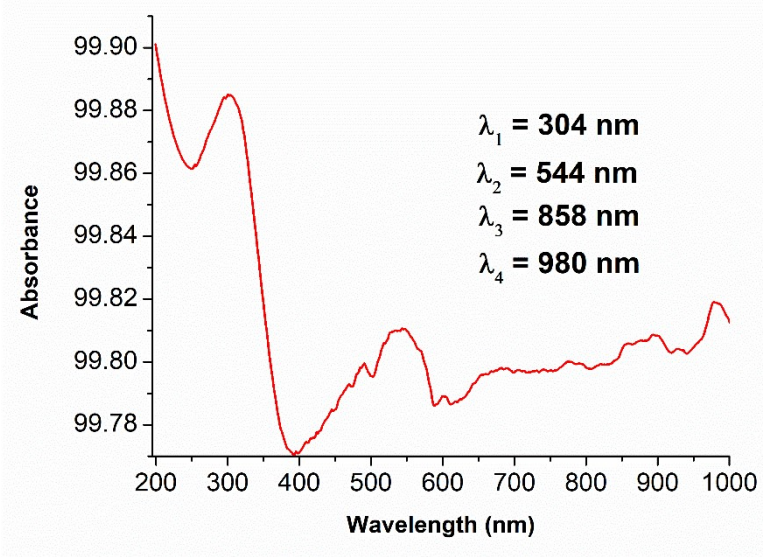

(a)

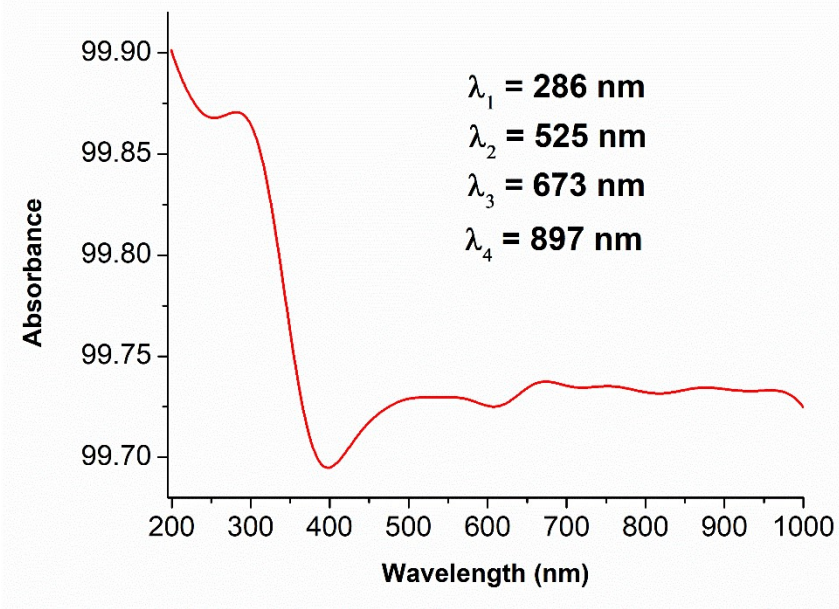

(b)

Figure S5. The UV-Vis spectra: (a) complex 1; (b) complex 2.

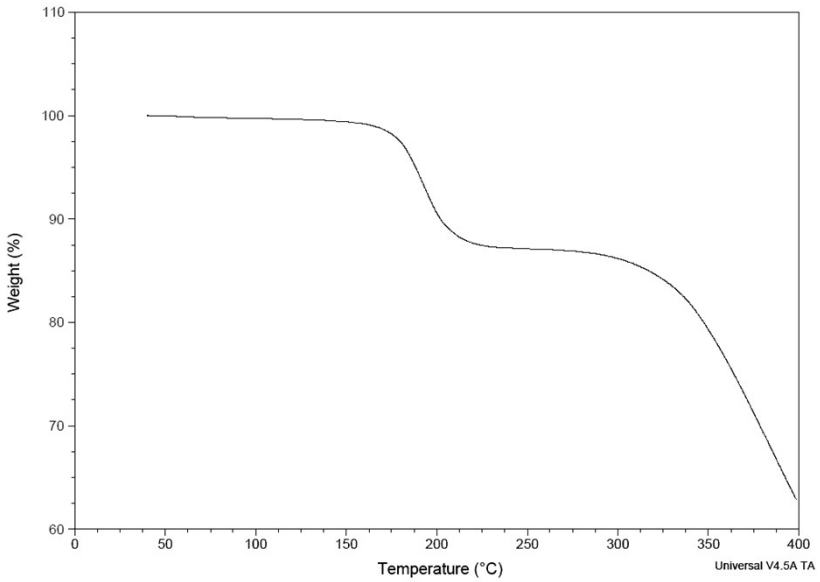

(a)

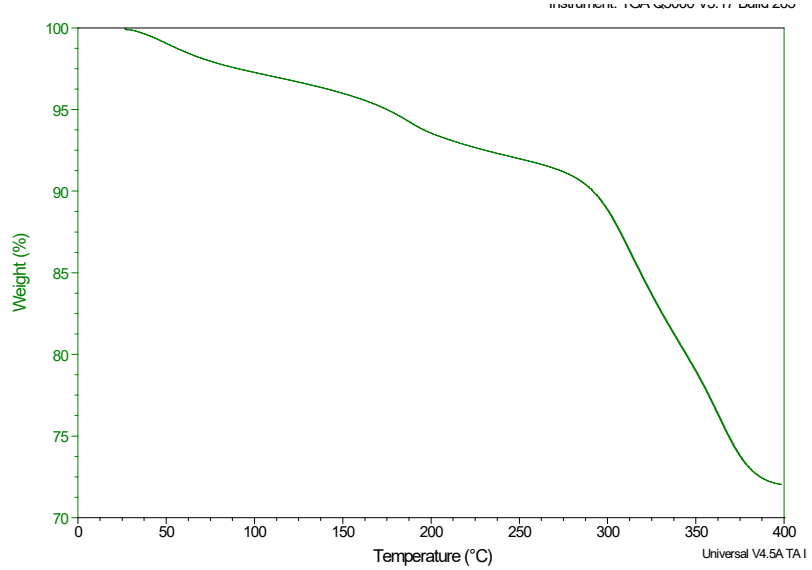

(b)

Figure S6 TGA traces of (a) **1** and (b) **2** in N_2.

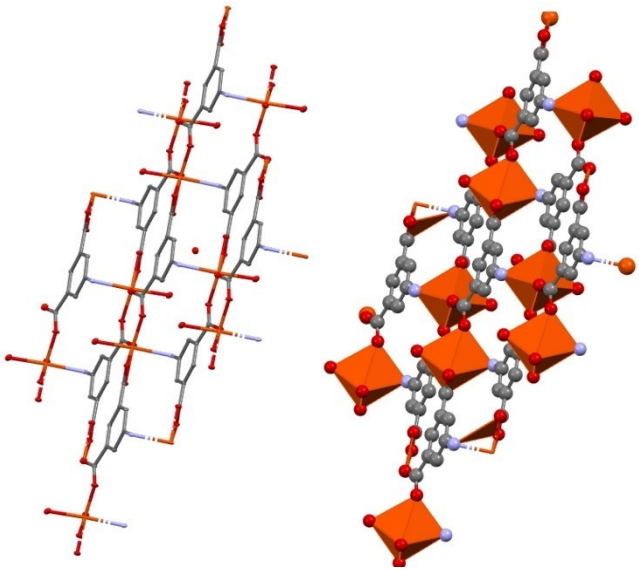

Figure S7 Mercury diagram 3D of **1** at the 50 % probability level, all H-atoms omitted for clarity. Color code: C, grey; N, blue; Fe, orange.

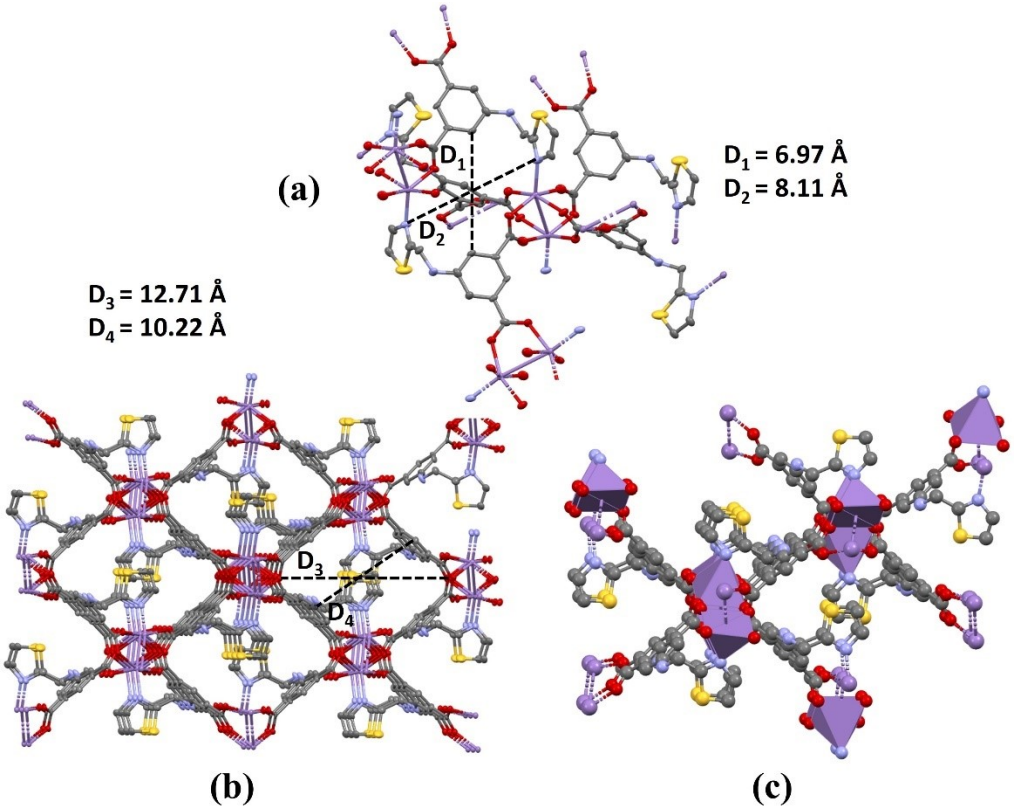

Figure S8 Mercury diagram of **5** at the probability 10 % level, all H-atoms omitted for clarity. Color code: C, grey; N, blue; O, red; Mn, purple; S, yellow.

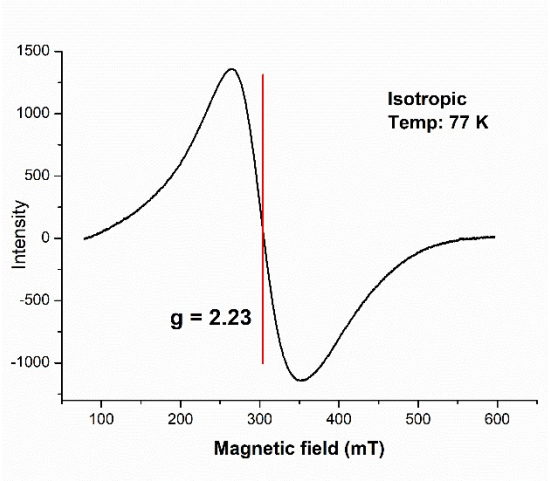
Isotropic
Temp: 77 K
g = 2.23
Intensity
Magnetic field (mT)

(a)

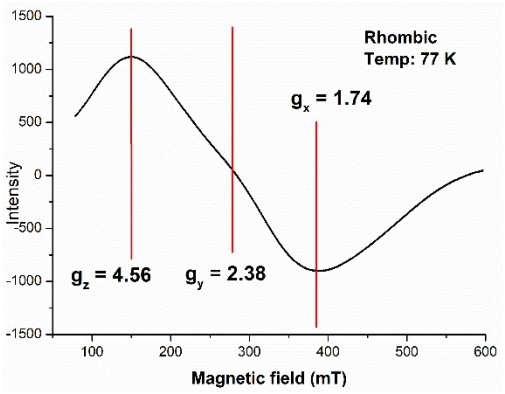
Rhombic
Temp: 77 K
g_x = 1.74
g_z = 4.56
g_y = 2.38
Intensity
Magnetic field (mT)

(b)

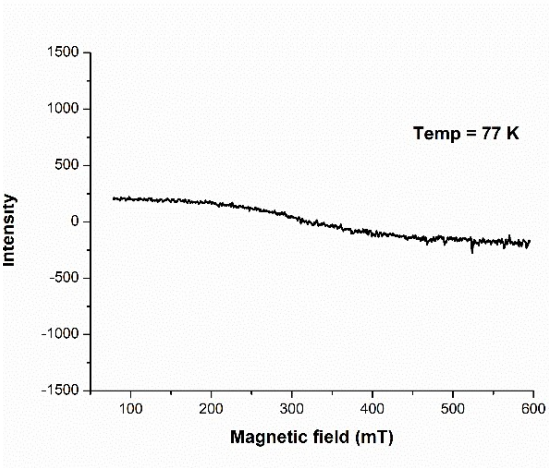
Temp = 77 K
Intensity
Magnetic field (mT)

(c)

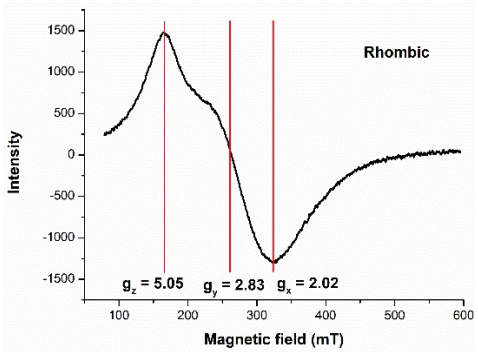

(d)

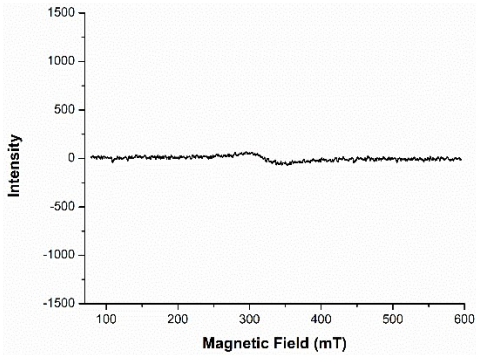

(e)

Figure S9 X-band ESR spectra collected at 77 K. (a) complex **1** (b) complex **2** (c) complex **3** (d) complex **4** (e) complex **5**.

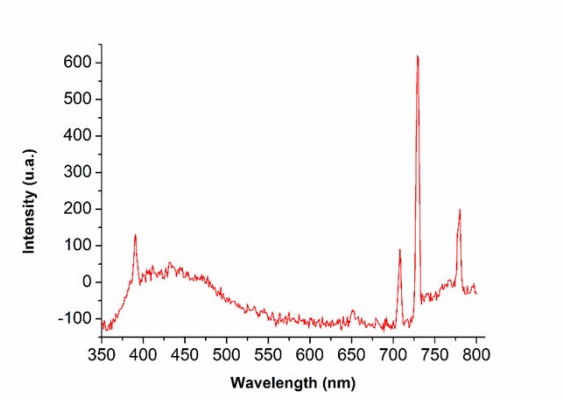

(a)

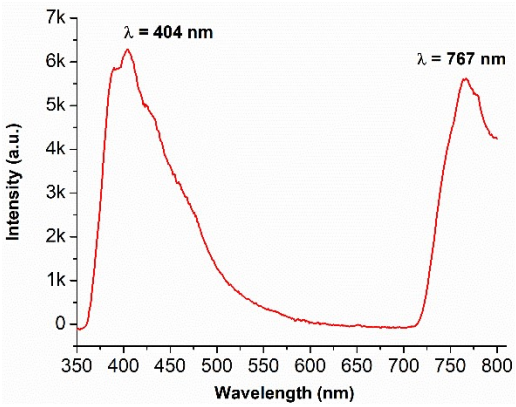

(b)

Figure S10. the excitation and emission spectra (a) complex **1** (b) complex **2**.

3. Electrodes Fabrication and Electrochemical Study

All electrochemical studies were carried out in a conventional three-electrode system with a platinum electrode, a glassy carbon, and a Calomel electrode 0.1 M KCl, V versus SHE +0.336 V[7] (CE) as the counter, working, and reference electrodes, respectively. Before electrochemical measurements, O_2 was purged out from the solution with argon. In cyclic voltammetry (CV) with CO_2, the support electrolyte (SE) solution was first purged with argon and then the purge switched to the gas of interest (CO_2), maintaining a constant flow to avoid the entry of O_2 into the electrochemical cell.

3.1 Preparation of the MOF-electrodes (ME) by depositing the material.

4 mg of the coordination polymer to be evaluated is macerated, until a very fine powder was obtained, then it was transferred to a glass vial and 2 mL of acetone was added, stirred vigorously for a period of 15 min. At the end of this time, the glassy carbon electrode is immersed in the suspension, to deposit a very thin layer of the MOF on the conductive surface of the electrode, finally allowed to dry at room temperature (Figure

S7, (a)).

3.2 Preparation of carbon paste electrodes.

19 mg of the coordination polymer to be evaluated were mixed with 47 mg of graphite and macerated until obtaining a very fine powder; then it was transferred to a glass vial and 2 or 3 drops of silicone oil were added, mixing to give a homogeneous paste, then packed in a plastic syringe tube of 5 mm in diameter (Figure S7, (b)); then it was cured at room temperature for a day. After this time a platinum filament was introduced to make the connection with the potentiostat (**Figure S11**).

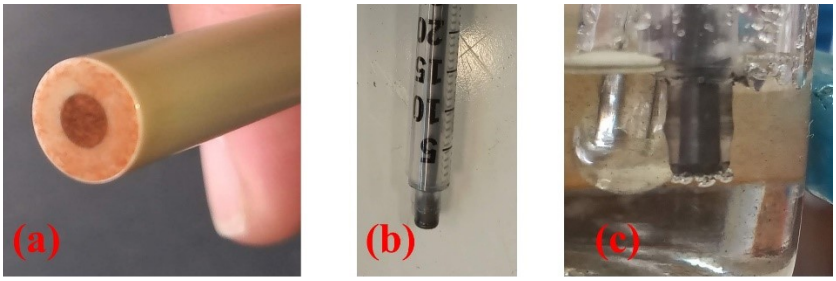

Figure S11. (a) MOF deposit on working electrode (b) carbon paste electrode (c) Bubbles generated during CV in the cathodic direction on the carbon paste electrode.

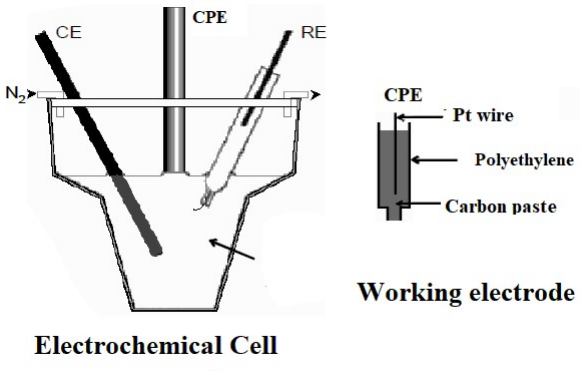

Figure S12. Configuration of the electrodes in an electrochemical cell for the Cyclic voltammetry and diagram of the carbon paste electrode (CPE). Where CE: counter electrode, RE: reference electrode.

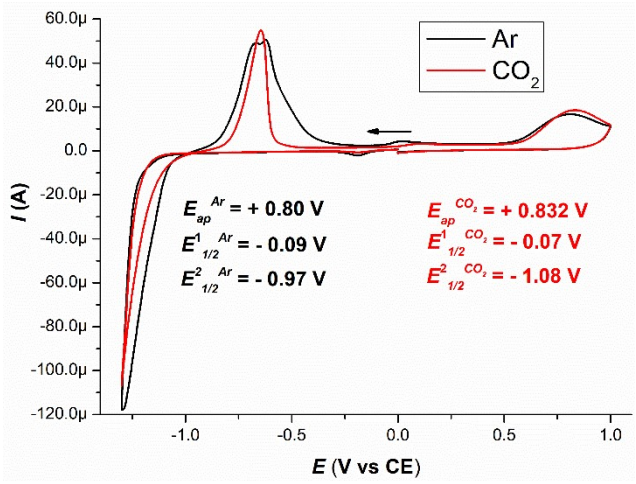
Ar
CO2
I (A)
E (V vs CE)
Eap Ar = + 0.80 V
E1/2 1 Ar = - 0.09 V
E1/2 2 Ar = - 0.97 V
Eap CO2 = + 0.832 V
E1/2 1 CO2 = - 0.07 V
E1/2 2 CO2 = - 1.08 V

(a)

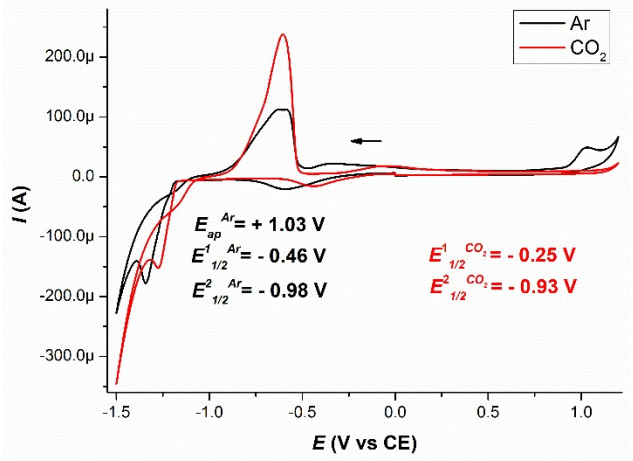
Ar
CO2
I (A)
E (V vs CE)
Eap Ar = + 1.03 V
E1/2 1 Ar = - 0.46 V
E1/2 2 Ar = - 0.98 V
E1/2 1 CO2 = - 0.25 V
E1/2 2 CO2 = - 0.93 V

(b)

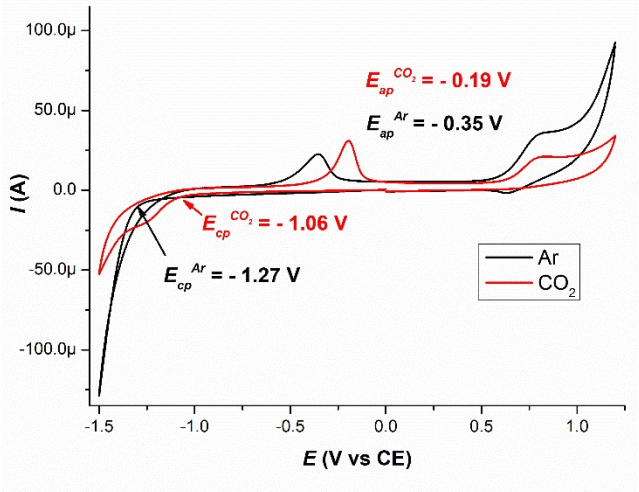
Eap CO2 = - 0.19 V
Eap Ar = - 0.35 V
Ecp CO2 = - 1.06 V
Ecp Ar = - 1.27 V
Ar
CO2
I (A)
E (V vs CE)

(c)

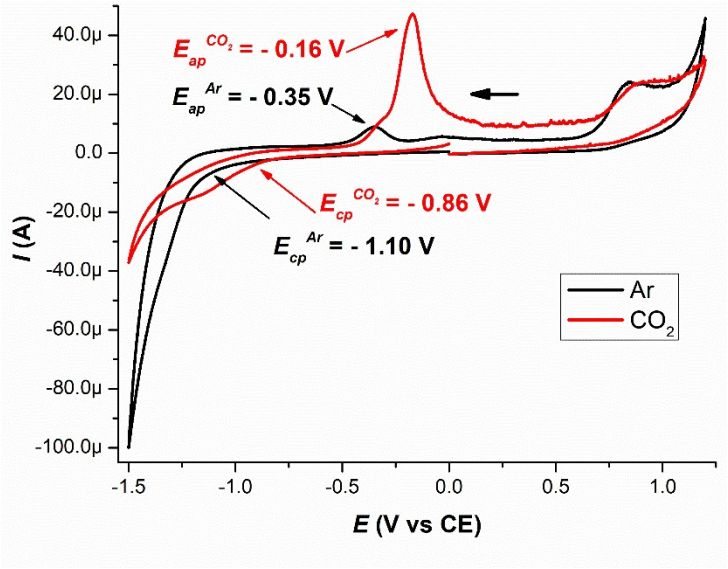

(d)

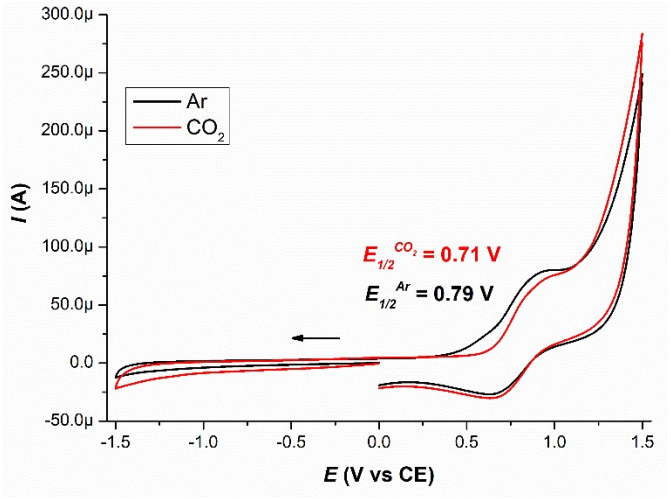

(e)

Figure S13. Cathodic cyclic voltammograms in 0.1 M KCl-H_2O at 100 mVs^{-1} scan rate, MOF-electrodes (ME) as working electrode. Red trace) atmosphere of carbon dioxide, blue trace) atmosphere of argon. (a) complex **1**, (b) complex **2**, (c) complex **3**, (d) complex **4**, (e) complex **5**.

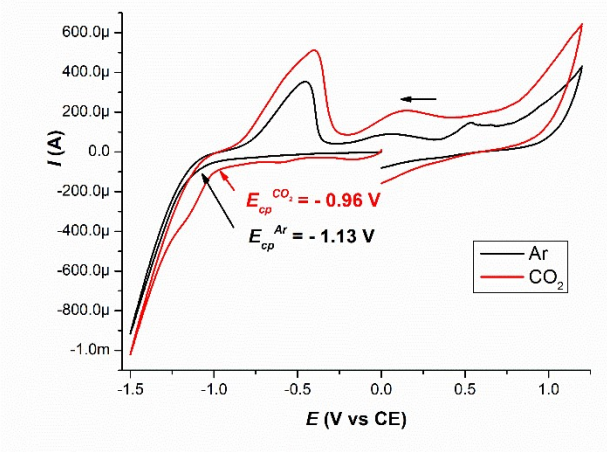

Figure S14. Cathodic cyclic voltammograms in 0.1 M KCl-H_2O at 100 mVs^{-1} scan rate, carbon paste electrode with complex **2** as working electrode. black trace) atmosphere of argon. red trace) atmosphere of carbon dioxide.

4. Qualitative CO detection test using Wilkinson's catalyst.

In a *Schlenk*-type flask, 25 mg of Wilkinson's catalyst was dissolved in anhydrous ethanol, under argon atmosphere, and the flask was closed with a rubber septum. Subsequently, the ethanolic solution is bubbled with the exit gases that come from chronoamperometry, for a period of 3 hours (**Figure S15**). After this time, the solution was dried under vacuum and the solid obtained was characterized by infrared spectroscopy. To be certain that the method used is the correct one trapping the carbon monoxide, tests were carried out by bubbling high purity CO in different solutions of the Wilkinson catalyst; one of the IR spectra of these solutions is shown in **Figure S15**, (c).

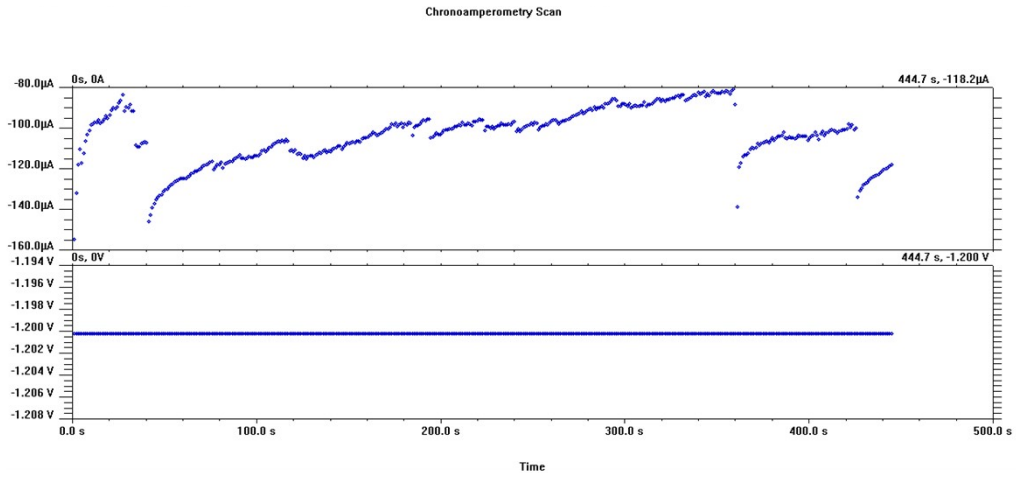

Figure S15 Image of the chronoamperometry performed to produce CO with the carbon paste electrode with complex **2**. Only a fraction of the experiment is shown. The release of gas bubbles from the surface of the electrode periodically makes the registered current value random, for this reason, a discontinuous graph is observed.

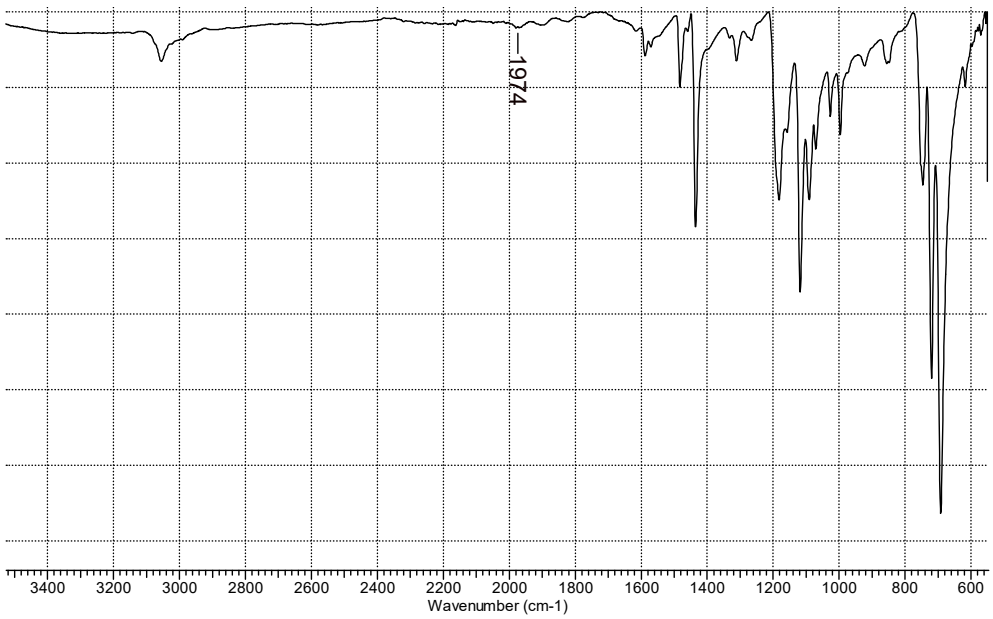

(a)

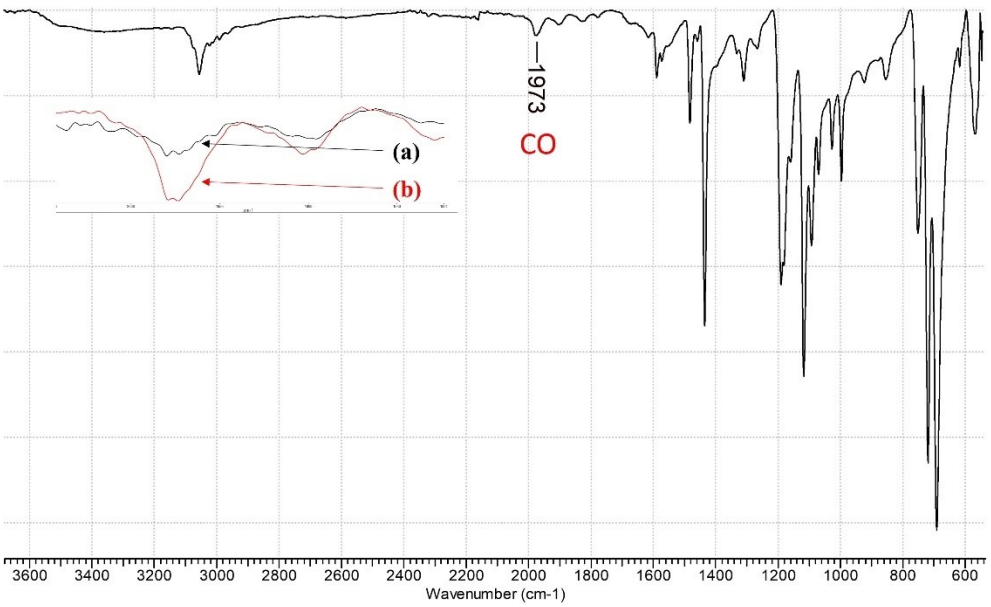

(b)

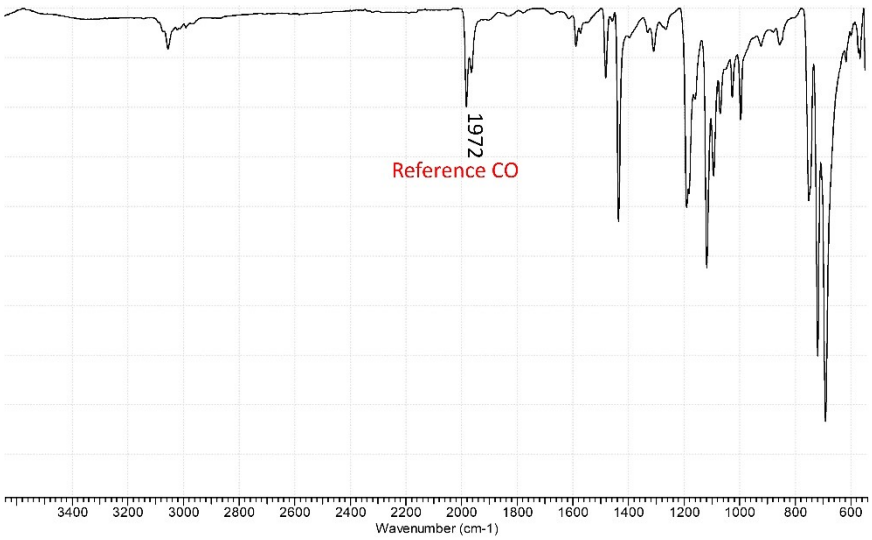

(c)

Figure S16. CO detection test. (a) Wilkinson complex before chronoamperometry. (b) Wilkinson complex after chronoamperometry, and (c) Wilkinson complex with CO.

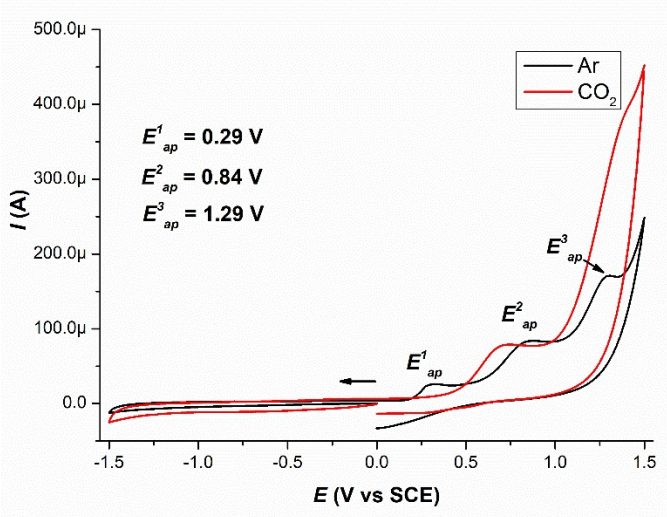

Figure S17. Cathodic cyclic voltammograms in 0.1 M $KHCO_3$-H_2O at 100 mVs^{-1} scan rate, MOF-electrodes (ME) as working electrode with complex **5** as working electrode. black trace) atmosphere of argon. red trace) atmosphere of carbon dioxide.

5 Calculation of the approximate amount of CO produced in chronoamperometry

A calibration curve was run with solid-state of Wilkinson catalyst (WC) standards, containing known amounts of Wilkinson catalyst that was exposed to carbon monoxide (WC-CO) (**Figure S16**, (c)). 12 standards were prepared that contained the WC-CO the following proportions: 0.00%, 4.75%, 14.04%, 20.00%, 35.85%, 47.36%, 67.77%, 70.40%, 77.66%, 83.08%, 92.00%, and 100%; these data were entered in the quantification method of the *Perkin-Elmer Spectrum Quant* software, version 10.6.2.1159. The IR spectra of the standards and the linearization equation of the method are shown in **Figure S17**.

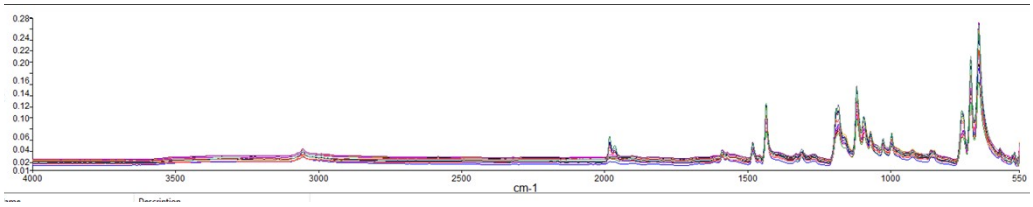

(a)

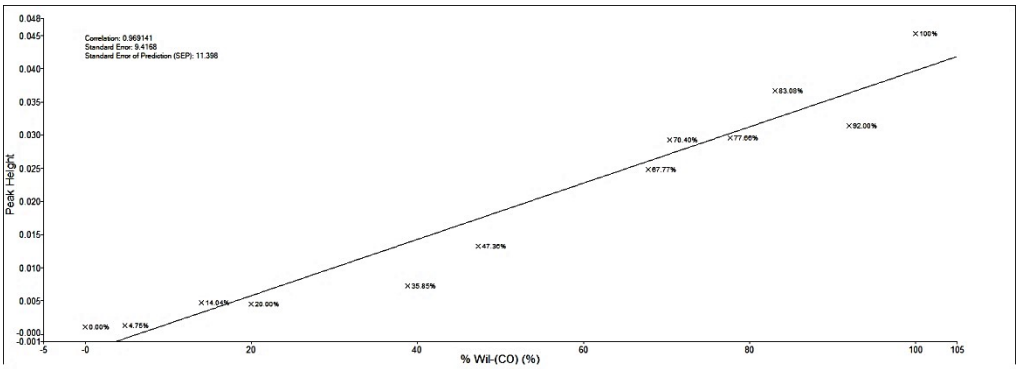

(b)

Figure S18 (a) IR spectra of the standards used in the CO quantification method. (b) Graph of the linearized method used to estimate the proportion of CO generated.

The estimated proportion of Wilkinson catalyst containing CO was 14.1 %. Hence, 4.57 mg CW-CO/25 mg CW. The calculation of faradic efficiency was carried out based on equation 1.

$$FE\ (\%) = (n_{pro} \bullet n_{e\text{-}}CO \bullet F) / Q \qquad \text{(Equation 1)}$$

Where n_{pro} is product moles, $n_{e\text{-}}CO$ is number of electrons for CO, F is a constant (96485 C mol^{-1}), and Q is the total charge passed during electrolysis.

Calculation of current density ***J***:

$$J\ (mA{\cdot}cm^{-2}) = I / A \qquad \text{(Equation 2)}$$

$$J = -\ 4.7\ mA{\cdot}cm^{-2}$$

Where I = - 0.141 mA, this was a value at the beginning of chronoamperometry, A = 0.03 cm^2 at -1.2 V.

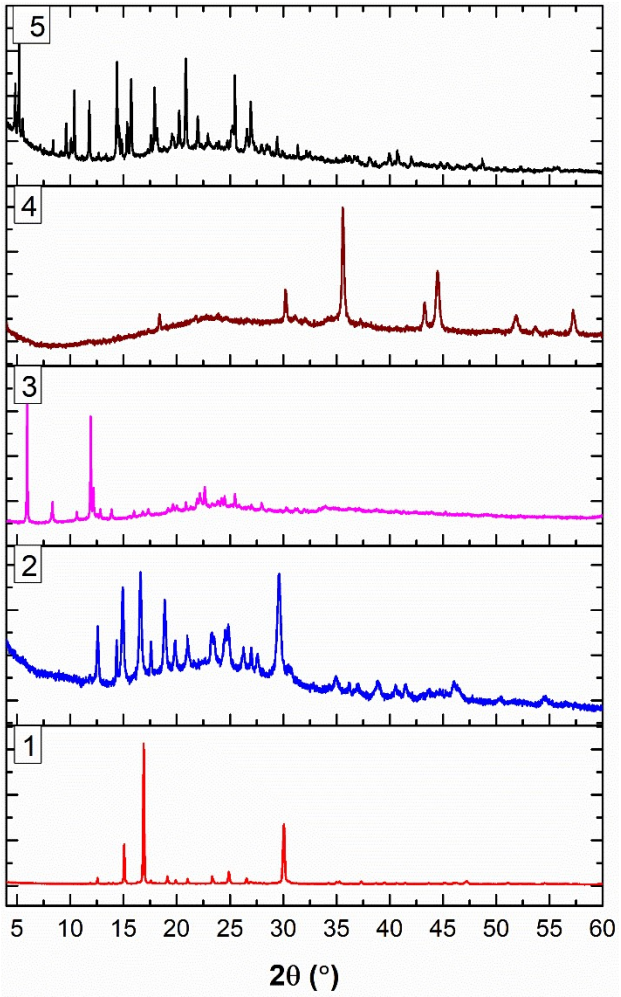

Figure S19. The PXRD spectra: (1) complex **1**; (2) complex **2**; (3) complex **3**; (4) complex **4**; (5) complex **5**.

References

[1] CrysAlisPRO and CrysAlisRED. Agilent Technologies, Agilent [2013]. Yarnton, England.
[2] R.C. Clark, J.S. Reid, *Acta Cryst.* **1995**, *A51*, 887.
[3] G.M Sheldrick, *Acta Crystallogr.* **2015**, *A71*, 3.
[4] G.M Sheldrick, *Acta Crystallogr.* **2015**, *C71*, 3.
[5] L.J. Farrugia, *J. Appl. Crystallogr.* **1999**, *32*, 837.
[6] C.F. Macrae, P.R. Edgington, P. McCabe, E. Pidcock, G.P. Shields, R. Taylor, M. Towler, *J. van de Streek, J. Appl. Crystallogr.* **2006**, *39*, 453.
[7] N. Eliaz, E. Gileadi, Physical Electrochemistry – Fundamentals, Techniques, and Applications, 2nd Edition, Wiley-VCH, 2019.